

Obtaining Wannier Functions of a Crystalline Insulator within a Hartree-Fock approach: applications to LiF and LiCl

Alok Shukla[†], Michael Dolg, Peter Fulde

*Max-Planck-Institut für Physik komplexer Systeme, Nöthnitzer Straße 38 D-01187 Dresden,
Germany*

Hermann Stoll

Institut für Theoretische Chemie, Universität Stuttgart, D-70550 Stuttgart, Germany

Abstract

An *ab initio* Hartree-Fock approach aimed at directly obtaining the localized orthogonal orbitals (Wannier functions) of a crystalline insulator is described in detail. The method is used to perform all-electron calculations on the ground states of crystalline lithium fluoride and lithium chloride, without the use of any pseudo or model potentials. Quantities such as total energy, x-ray structure factors and Compton profiles obtained using the localized Hartree-Fock orbitals are shown to be in excellent agreement with the corresponding quantities calculated using the conventional Bloch-orbital based Hartree-Fock approach. Localization characteristics of these orbitals are also discussed in detail.

I. INTRODUCTION

Electronic-structure calculations on periodic systems are conventionally done using the so-called Bloch orbital based approach which consists of assuming an itinerant form for the single-electron wave functions. This approach has the merit of incorporating the translational invariance of the system under consideration, as well as its infinite character, in an elegant and transparent manner. An alternative approach to electronic-structure calculations on periodic systems was proposed by Wannier¹. In this approach, instead of describing the electrons in terms of itinerant Bloch orbitals, one describes them in terms of mutually orthogonal orbitals localized on individual atoms or bonds constituting the infinite solid. Since then such orbitals have come to be known as Wannier functions. It can be shown that the two approaches of description of an infinite solid are completely equivalent and that the two types of orbitals are related by a unitary transformation². Therefore, the two approaches differ only in terms of their practical implementation. However, the description of metallic systems in terms of Wannier functions frequently runs into problems as it is found that for such systems the decay of the orbitals away from the individual atomic sites is of power law type and not of exponential type. In other words, the Wannier functions for such systems are not well localized². This behavior is to be expected on intuitive grounds as electrons in metals are indeed quite delocalized. On the other hand, for the situations involving surfaces, impurity states, semiconductors and insulators, where the atomic character of electrons is of importance, Wannier functions offer a natural description.

Recent years have seen an increased amount of activity in the area of solid-state calculations based on localized orbitals³, of which Wannier functions are a subclass. Most of these approaches have been proposed with the aim of developing efficient order-N methods for electronic structure calculations on solids within the framework of density functional theory. With a different focus, Nunes and Vanderbilt⁴ have developed an entirely Wannier-function based approach to electronic-structure calculations on solids in the presence of electric fields, a case for which the eigenstates of the Hamiltonian are no longer Bloch states. However,

we believe that there is one potential area of application for Wannier orbitals which remains largely unexplored, namely in the *ab initio* treatment of electron-correlation effects in solids using the conventional quantum-chemical methods⁵. It is intuitively obvious that an *ab initio* treatment of electron correlations on large systems will converge much faster with localized orbitals as compared to delocalized orbitals because the Coulomb repulsion between two electrons will decay rapidly with the increasing distance between the electrons. In the quantum-chemistry community the importance of localized orbitals in treating the correlation effects in large systems was recognized early on and various procedures aimed at obtaining localized orbitals were developed⁶. Some of the localized-orbital approaches were also carried over to solids chiefly by Kunz and collaborators⁷ at the Hartree-Fock level. This approach has been applied to a variety of systems⁸. Kunz, Meng and Vail⁹ have gone beyond the Hartree-Fock level and also included the influence of electron correlations for solids using many-body perturbation theory. The scheme of Kunz et al. is based upon nonorthogonal orbitals which, in general, are better localized than their orthogonal counterparts. However, the subsequent treatment of electron correlations with nonorthogonal orbitals is generally much more complicated than the one based upon true Wannier functions.

In our group electron correlation effects on solids have been studied using the incremental scheme of Stoll¹⁰ which works with localized orbitals. In such studies the infinite solid is modeled as a large enough cluster and then correlation effects are calculated by incrementally correlating the Hartree-Fock reference state of the cluster expressed in terms of localized orbitals¹¹. However, a possible drawback of this procedure is that there will always be finite size effects and no *a priori* knowledge is available as to the difference in results when compared with the infinite-solid limit. In order to be able to study electron-correlation effects in the infinite-solid limit using conventional quantum-chemical approaches, one first has to obtain a Hartree-Fock representation of the system in terms of Wannier functions. This task is rather complicated because, in addition to the localization requirement, one also imposes the constraint upon the Wannier functions that they be obtained by the Hartree-Fock minimization of the total energy of the infinite solid. In an earlier paper¹²—henceforth

referred to as I—we had outlined precisely such a procedure which obtained the Wannier functions of an infinite insulator within a Hartree-Fock approach and reported its preliminary applications to the lithium hydride crystal. In the present paper we describe all theoretical and computational details of the approach and report applications to larger systems namely lithium fluoride and lithium chloride. Unlike I, where we only reported results on the total energy per unit cell of the system, here we also use the Hartree-Fock Wannier functions to compute the x-ray structure factors and Compton profiles. Additionally, we also discuss the localization characteristics of the Wannier functions in detail. All the physical quantities computed with our procedure are found to be in excellent agreement with those computed using the CRYSTAL program¹³ which employs a Bloch orbital based *ab initio* Hartree-Fock approach. In a future publication we will apply the present formalism to perform *ab initio* correlation calculations on an infinite insulator.

The rest of this paper is organized as follows. In section II we develop the theoretical formalism at the Hartree-Fock level by minimizing the corresponding energy functional, coupled with the requirement of translational symmetry, and demonstrate that the resulting HF equations correspond to the HF equations for a unit cell of the solid embedded in the field of identical unit cells constituting the rest of the infinite solid. Thus an embedded-cluster picture for the infinite solid emerges rigorously from this derivation. Subsequently a localizing potential is introduced in the HF equations by means of projection operators leading to our working equations for the Hartree-Fock Wannier orbitals for an infinite solid. Finally, these equations are cast in the matrix form using a linear combination of atomic orbitals approach which is used in the actual calculations. In section III we present the results of our calculations performed using the aforementioned formalism on LiF and LiCl crystals. Finally, in section IV we present our conclusions. Various aspects related to the computer implementation of the present approach are discussed in the appendix.

II. THEORY

A. Hartree-Fock Equations

We consider the case of a perfect solid without the presence of any impurities or lattice deformations such as phonons. We also ignore the effects of relativity completely so that the spin-orbit coupling is also excluded. In such a case, in atomic units¹⁴, the nonrelativistic Hamiltonian of the system consisting of the kinetic energy of electrons, electron-nucleus interaction, electron-electron repulsion and nucleus-nucleus interaction is given by

$$H = -\frac{1}{2} \sum_i \nabla_i^2 - \sum_i \sum_I \frac{Z_I}{|\mathbf{r}_i - \mathbf{R}_I|} + \sum_{i>j} \frac{1}{|\mathbf{r}_i - \mathbf{r}_j|} + \sum_{I>J} \frac{Z_I Z_J}{|\mathbf{R}_I - \mathbf{R}_J|}, \quad (1)$$

where in the equation above \mathbf{r}_i denotes the position coordinates of the i -th electron while \mathbf{R}_I and Z_I respectively denote the position and the charge of the I -th nucleus of the lattice. For a given geometry of the solid the last term representing the nucleus-nucleus interaction will make a constant contribution to the energy and will not affect the dynamics of the electrons. To develop the theory further we make the assumptions that the solid under consideration is a closed-shell system and that a single Slater determinant represents a reasonable approximation to its ground state. Moreover, we assume that the same spatial orbitals represent both the spin projections of a given shell, i.e., we confine ourselves to restricted Hartree-Fock (RHF) theory. With the preceding assumptions, the total energy of the solid can be written as

$$E_{solid} = 2 \sum_i \langle i|T|i \rangle + 2 \sum_i \langle i|U|i \rangle + \sum_{i,j} (2 \langle ij|ij \rangle - \langle ij|ji \rangle) + E_{nuc}, \quad (2)$$

where $|i \rangle$ and $|j \rangle$ denote the occupied spatial orbitals assumed to form an orthonormal set, T denotes the kinetic energy operator, U denotes the electron-nucleus potential energy, E_{nuc} denotes the nucleus-nucleus interaction energy and $\langle ij|ij \rangle$ etc. represent the two-electron integrals involving the electron repulsion. The equation above is completely independent of the spin degree of freedom which, in the absence of spin-orbit coupling, can be summed away leading to familiar factors of two in front of different terms. Clearly the terms involving $\langle i|U|i \rangle$, $\langle ij|ij \rangle$, and E_{nuc} contain infinite lattice sums and are convergent

only when combined together. So far the energy expression of Eq.(2) does not incorporate any assumptions regarding the translational symmetry of a perfect solid. In keeping with our desire to introduce translational symmetry in the real space, without having to invoke the \mathbf{k} -space as is usually done in the Bloch orbital based theories, we make the following observation. A crystalline solid, in its ground state, is composed of identical unit cells and the orbitals belonging to a given unit cell are identical to the corresponding orbitals belonging to any other unit cell and are related to one another by a simple translation operation. Assuming that the number of orbitals in a unit cell is n_c and if we denote the α -th orbital of a unit cell located at the position given by the vector \mathbf{R}_j of the lattice by $|\alpha(\mathbf{R}_j) \rangle$ then clearly the set $\{|\alpha(\mathbf{R}_j) \rangle; \alpha = 1, n_c; j = 1, N\}$ denotes all the orbitals of the solid. In the previous expression N is the total number of unit cells in the solid which, of course, is infinite. Henceforth, Greek labels $\alpha, \beta, \gamma, \dots$ will always denote the orbitals of a unit cell. The translational symmetry condition expressed in the real space can be stated simply as

$$|\alpha(\mathbf{R}_i + \mathbf{R}_j) \rangle = \mathcal{T}(\mathbf{R}_i)|\alpha(\mathbf{R}_j) \rangle, \quad (3)$$

where $\mathcal{T}(\mathbf{R}_i)$ is an operator which represents a translation by vector \mathbf{R}_i . Using this, one can rewrite the energy expression of Eq.(2) as

$$E = N \left\{ 2 \sum_{\alpha=1}^{n_c} \langle \alpha(o) | T | \alpha(o) \rangle + 2 \sum_{\alpha=1}^{n_c} \langle \alpha(o) | U | \alpha(o) \rangle + \sum_{\alpha, \beta=1}^{n_c} \sum_{j=1}^N (2 \langle \alpha(o) \beta(\mathbf{R}_j) | \alpha(o) \beta(\mathbf{R}_j) \rangle - \langle \alpha(o) \beta(\mathbf{R}_j) | \beta(\mathbf{R}_j) \alpha(o) \rangle) + e_{nuc} \right\}, \quad (4)$$

where $|\alpha(o) \rangle$ denotes an orbital centered in the reference unit cell, e_{nuc} involves the interaction energy of the nuclei of the reference cell with those of the rest of the solid ($E_{nuc} = N e_{nuc}$), and we have removed the subscript *solid* from the energy. The preceding equation also assumes the important fact that the orbitals obtained by translation operation of Eq.(3) are orthogonal to each other. We shall elaborate this point later in this section. An important simplification to be noted here is that by assuming the translational invariance in real space as embodied in Eq.(3), we have managed to express the total Hartree-Fock energy of the infinite solid in terms of a finite number of orbitals, namely the orbitals of a unit cell n_c . If

we require that the energy of Eq.(4) be stationary with respect to the first-order variations in the orbitals, subject to the orthogonality constraint, we are led to the Hartree-Fock operator

$$H_{HF} = T + U + 2 \sum_{\beta} J_{\beta} - \sum_{\beta} K_{\beta} \quad (5)$$

where J and K —the conventional Coulomb and exchange operators, respectively—are defined as

$$\left. \begin{aligned} J_{\beta}|\alpha > &= \sum_j < \beta(\mathbf{R}_j) | \frac{1}{r_{12}} | \beta(\mathbf{R}_j) > |\alpha > \\ K_{\beta}|\alpha > &= \sum_j < \beta(\mathbf{R}_j) | \frac{1}{r_{12}} | \alpha > | \beta(\mathbf{R}_j) > \end{aligned} \right\}. \quad (6)$$

Any summation over Greek indices $\alpha, \beta, \gamma, \dots$ will imply summation over all the n_c orbitals of a unit cell unless otherwise specified. As mentioned earlier, the terms U , J and K involve infinite lattice sums and their practical evaluation will be discussed in the next section. The eigenvectors of the Hartree-Fock operator of Eq.(5) will be orthogonal to each other, of course. However, in general, these solutions would neither be localized, nor would they be orthogonal to the orbitals of any other unit cell. This is because the orbitals centered in any other unit cell are obtained from those of the reference cell using a simple translation operation as defined in Eq.(3), which does not impose any orthogonality or localization constraint upon them. Since our aim is to obtain the Wannier functions of the infinite solid, i.e., all the orbitals of the solid must be localized and orthogonal to each other, we will have to impose these requirements explicitly upon the eigenspace of (5). This can most simply be accomplished by including in (5) the projection operators corresponding to the orbitals centered in the unit cells in a (sufficiently large) neighborhood of the reference cell

$$(T + U + 2J - K + \sum_{k \in \mathcal{N}} \sum_{\gamma} \lambda_{\gamma}^k |\gamma(\mathbf{R}_k) > < \gamma(\mathbf{R}_k)|) |\alpha > = \epsilon_{\alpha} |\alpha >, \quad (7)$$

where $|\alpha >$ stands for $|\alpha(o) >$, an orbital centered in the reference unit cell, $J = \sum_{\beta} J_{\beta}$, $K = \sum_{\beta} K_{\beta}$, and \mathcal{N} collectively denotes the unit cells in the aforementioned neighborhood. Clearly the choice of \mathcal{N} will be dictated by the system under consideration—the more delocalized electrons of the system are, the larger will \mathcal{N} need to be. In our calculations we have typically chosen \mathcal{N} to include up to third nearest-neighbor unit cells of the reference

cell. In the equation above λ_γ^k 's are the shift parameters associated with the corresponding orbitals of \mathcal{N} . For perfect orthogonality and localization, their values should be infinitely high. By setting the shift parameters λ_γ^k 's to infinity we in effect raise the orbitals localized in the environment unit cells (region \mathcal{N}) to very high energies compared to those localized in the reference cell. Thus the lowest energy solutions of Eq.(7) will be the ones which are localized in the reference unit cell and are orthogonal to the orbitals of the environment cells. Of course, in practice, it suffices to choose a rather large value for these parameters, and the issue pertaining to this numerical choice is discussed further in section III. Eq.(7) will generally be solved iteratively as described in the next section. If the initial guesses for the orbitals of the unit cell $\{|\alpha\rangle, \alpha = 1, n_c\}$ are localized, subsequent orthogonalization by means of projection operators will not destroy that property⁶ and the final solutions of the problem will be localized orthogonal orbitals. Therefore, projection operators along with the shift parameters, simply play the role of a localizing potential⁶ as it is clear that upon convergence their contribution to the Hartree-Fock equation vanishes. The orbitals contained in unit cells located farther than those in \mathcal{N} should be automatically orthogonal to the reference cell orbitals by virtue of the large distance between them. It is clear that the orthogonalization of the orbitals to each other will introduce oscillations in these orbitals which are also referred to as the orthogonalization tails.

Combining the orthogonality of the neighboring orbitals to the reference cell orbitals with the translation symmetry of the infinite solid, it is easy to see that the orbitals of any unit cell are orthogonal to all the orbitals of the rest of the unit cells. Therefore, orbitals thus obtained are essentially Wannier functions. After solving for the HF equations presented above one can obtain the electronic part of the energy per unit cell simply by dividing the total energy of Eq.(4) by N , which, unlike the total energy, is a finite quantity.

In paper I we arrived at exactly the same HF equations as above, although we had followed a more intuitive path utilizing the so-called “embedded-cluster” philosophy, whereby we minimized only that portion of the total energy of Eq.(2) which corresponds to the “cluster-environment” interaction. The fact that the derivations reported in paper I, and

here, both lead to the same final equations has to do with the translation invariance which allows the total energy to be expressed in the form of Eq.(4). Therefore, we emphasize that the equations derived above are exact and do not involve any approximation other than the Hartree-Fock approximation itself. Thus results of all the computations utilizing this approach should be in complete agreement with the equivalent computations performed using the traditional Bloch orbital based approach as is implemented, e.g, in the program CRYSTAL¹³.

By inspection of Eq.(7) it is clear that it is of the embedded-cluster form in the sense that if one calls the reference unit cell the “central cluster”, it describes the dynamics of the electrons of this central cluster embedded in the field of identical unit cells of its environment (rest of the infinite solid).

B. Linear Combination of Atomic Orbital Implementation

We have performed a computer implementation of the formalism presented in the previous section within a linear combination of atomic orbital (LCAO) approach, whereby we transform the differential equations of Eq.(7) into a set of linear equations solvable by matrix methods. Atomic units were used throughout the numerical work. We proceed by expanding the orbitals localized in the reference cell as

$$|\alpha\rangle = \sum_p \sum_{\mathbf{R}_j \in \mathcal{C} + \mathcal{N}} C_{p,\alpha} |p(\mathbf{R}_j)\rangle, \quad (8)$$

where \mathcal{C} has been used to denote the reference cell, \mathbf{R}_j represents the location of the j th unit cell (located in \mathcal{C} or \mathcal{N}) and $|p(\mathbf{R}_j)\rangle$ represents a basis function centred in the j th unit cell. In order to account for the orthogonalization tails of the reference cell orbitals, it is necessary to include the basis functions centred in \mathcal{N} as well. Clearly, the translational symmetry of the crystal as expressed in Eq.(3) demands that the orbitals localized in two different unit cells have the same expansion coefficients $C_{p,\alpha}$, and differ only in the location of the centers of the basis functions. The LCAO formalism implemented in most of the quantum-chemistry

molecular programs, as also in the CRYSTAL code¹³, expresses the basis functions $|p(\mathbf{R}_j) \rangle$ of Eq.(8) as linear combinations of Cartesian Gaussian type basis functions (CGTFs) of the form

$$\phi(\mathbf{r}, \eta_p, \mathbf{n}, \mathbf{R}) = (x - R_x)^{n_x} (y - R_y)^{n_y} (z - R_z)^{n_z} \exp(-\eta_p (\mathbf{r} - \mathbf{R})^2), \quad (9)$$

where $\mathbf{n} = (n_x, n_y, n_z)$. In the previous equation, η_p denotes the exponent and the vector \mathbf{R} represents the center of the basis function. The centers of the basis functions \mathbf{R} are normally taken to be at the locations of the appropriate atoms of the system. CGTFs with $n_x + n_y + n_z = 0, 1, 2, \dots$ are called respectively *s, p, d*... type basis functions¹⁵. The individual basis functions of the form of Eq.(9) are called *primitive* functions while the linear combinations of them are called the *contracted* functions. The formalism is totally independent of the type of basis functions, but for the sake of computational simplicity, we have programmed our approach using Gaussian lobe-type functions¹⁶. In this approach one approximates the *p* and higher angular momentum CGTFs as linear combinations of *s*-type basis functions displaced by a small amount from the location of the atom concerned. For example, in the present study a primitive *p* type CGTF centered at the origin was approximated as

$$\phi_p(\mathbf{r}, \eta) = A \{ \exp(-\eta(\mathbf{r} + \mathbf{d}_\eta)^2) - \exp(-\eta(\mathbf{r} - \mathbf{d}_\eta)^2) \}, \quad (10)$$

where, A is the normalization constant and $|\mathbf{d}_\eta| = C/\sqrt{\eta}$. In the present study the value of 0.1 atomic units (a.u.) was employed for C . For approximating the p_x, p_y and p_z types of basis functions, the displacement vectors \mathbf{d}_η are chosen to be along the positive x, y and z directions, respectively. By substituting Eq.(8) in Eq.(7) we obtain the HF equations in the LCAO matrix form

$$\sum_q F_{pq} C_{q,a} = \epsilon_a \sum_q S_{pq} C_{q,a}. \quad (11)$$

The Fock matrix F_{pq} occurring in the equation above is defined as

$$F_{pq} = \langle p | (T + U + 2J - K) | q \rangle + \sum_{k \in \mathcal{N}} \sum_{\gamma} \sum_{p', q'} \lambda_{\gamma}^k S_{pp'} S_{qq'} C_{p', \gamma} C_{q', \gamma}, \quad (12)$$

where the contribution of all the operators appearing in Eq.(7) has been replaced by the corresponding matrices in the representation of the chosen basis set. Above, unprimed functions $|p\rangle$ and $|q\rangle$ represent the basis functions corresponding to the orbitals of the reference unit cell while the primed functions $|p'\rangle$ and $|q'\rangle$ denote the basis functions corresponding to the orbitals of \mathcal{N} . In particular, the overlap matrix is given by

$$S_{pq} = \langle p|q \rangle \quad (13)$$

and the Coulomb and the exchange matrix elements are defined as

$$\langle p|J|q \rangle = \sum_{r,s} \sum_k \langle p r(\mathbf{R}_k) | \frac{1}{r_{12}} | q s(\mathbf{R}_k) \rangle D_{rs} \quad (14)$$

and

$$\langle p|K|q \rangle = \sum_{r,s} \sum_k \langle p r(\mathbf{R}_k) | \frac{1}{r_{12}} | s(\mathbf{R}_k) q \rangle D_{rs}, \quad (15)$$

where D_{rs} denotes the elements of the density matrix D of the orbitals of a unit cell evaluated as¹⁷

$$D_{pq} = \sum_{\alpha} C_{p,\alpha} C_{q,\alpha}. \quad (16)$$

The matrix form of the HF equations (11) is a pseudo eigenvalue problem which can be solved iteratively to obtain the HF orbitals. The energy per unit cell can be computed by means of a simple matrix-trace operation

$$E_{cell} = Tr\{(2T + 2U + 2J - K)D\} + e_{nuc}, \quad (17)$$

where above T , U , J and K and D denote the matrices of the corresponding operators in the representation of the chosen basis set, and e_{nuc} was defined after Eq.(4).

In practice one proceeds according to the following algorithm:

1. Start with some localized initial guess for the orbitals of the reference cell. For ionic systems considered here we chose these to be the orbitals of the individual ions centered on the corresponding atomic sites. For covalent systems, it would be reasonable to use suitable bonding combinations of atomic orbitals.

2. Use these orbitals to construct the Fock matrix as defined in Eq.(12).
3. Diagonalize the Fock matrix to obtain a new set of orbitals of the reference cell.
4. Compute the energy per unit cell by using Eq.(17).
5. Go to step 2. Iterate until the energy per unit cell has converged.

Various mathematical formulas and computational aspects related to the evaluation of different contributions to the Fock matrix are discussed in the appendix.

C. Evaluation of Properties

In this section we describe the evaluation of the x-ray structure factors and Compton profiles from the Hartree-Fock Wannier functions obtained from the formalism of the previous section. Both these properties can be obtained from the first-order density matrix of the system defined for the present case as

$$\rho(\mathbf{r}, \mathbf{r}') = 2 \sum_i \sum_{\alpha} \phi_{\alpha}(\mathbf{r} - \mathbf{R}_i) \phi_{\alpha}^*(\mathbf{r}' - \mathbf{R}_i) \quad (18)$$

where $\phi_{\alpha}(\mathbf{r} - \mathbf{R}_i) = \langle \mathbf{r} | \alpha(\mathbf{R}_i) \rangle$ is the α -th HF orbital of the unit cell located at position \mathbf{R}_i . The factor of two above is a consequence of spin summation.

1. X-ray Structure Factors

By measuring the x-ray structure factors experimentally one can obtain useful information on the charge density of the constituent electrons. Theoretically, the x-ray structure factor $S(\mathbf{k})$ can be obtained by taking the Fourier transform of the diagonal part of the first-order density matrix

$$S(\mathbf{k}) = \int \rho(\mathbf{r}, \mathbf{r}) \exp(i\mathbf{k} \cdot \mathbf{r}) d\mathbf{r} \quad (19)$$

2. Compton Profile

By means of Compton scattering based experiments, one can extract the information on the momentum distribution of the electrons of the solid. In the present study we compute the Compton profile in the impulse approximation as developed by Eisenberger and Platzman¹⁸. Under the impulse approximation the Compton profile for the momentum transfer q is defined as¹⁸

$$J(q) = \frac{1}{(2\pi)^3} \int \delta(\omega - \frac{k^2}{2m} - \frac{q}{m}) M(\mathbf{p}) d\mathbf{p}, \quad (20)$$

where \mathbf{k} and ω are, respectively, the changes in momentum and the frequency of the incoming x- or γ -ray due to scattering, \mathbf{p} is the Compton electron momentum, $q = \frac{\mathbf{k} \cdot \mathbf{p}}{k}$ is the projection of \mathbf{p} in the direction of \mathbf{k} , the delta function imposes the energy conservation and $M(\mathbf{p}) = \rho(\mathbf{p}, \mathbf{p})$ denotes the electron momentum distribution obtained from the diagonal part of the full Fourier transform of the first-order density matrix

$$\rho(\mathbf{p}, \mathbf{p}') = \int \exp(i(\mathbf{p} \cdot \mathbf{r} - \mathbf{p}' \cdot \mathbf{r}')) \rho(\mathbf{r}, \mathbf{r}') d\mathbf{r} d\mathbf{r}'. \quad (21)$$

By choosing the z -axis of the coordinate system defining \mathbf{p} along the direction of \mathbf{k} , one can perform the p_z integral in Eq.(20) to yield

$$J(q) = \frac{1}{(2\pi)^3} \int_{-\infty}^{\infty} dp_x \int_{-\infty}^{\infty} dp_y M(p_x, p_y, q), \quad (22)$$

Integrals contained in the expressions for the x-ray structure factor and the Compton profile (Eqs. (19) and (22), respectively) can be performed analytically when the density matrix is represented in terms of Gaussian lobe-type basis functions. These analytic expressions are used to evaluate the quantities of interest in our computer code, once the Hartree-Fock density matrix has been determined.

III. CALCULATIONS AND RESULTS

In this section we present the results of the calculations performed on crystalline LiF and LiCl. Prencipe et al.¹⁹ studied these compounds, along with several other alkali halides,

using the CRYSTAL program¹³. CRYSTAL, as mentioned earlier, is a Bloch orbital based *ab initio* Hartree-Fock program set up within an LCAO scheme, utilizing CGTFs as basis functions. In their study, Prencipe et al. employed a very large basis set and, therefore, their results are believed to be very close to the Hartree-Fock limit. In the present work our intention is not to repeat the extensive calculations of Prencipe et al.¹⁹, but rather to demonstrate that at the Hartree-Fock level one can obtain the same physical insights by applying the Wannier function based approach as one would by utilizing the Bloch orbital based approach. Moreover, because of the use of lobe functions as basis functions, we run into problems related to numerical instability when very diffuse *p*-type (and beyond) basis functions are employed. In future we intend to incorporate true CGTFs as basis functions in our program, which should make the code numerically much more stable. Therefore, we have performed these calculations with modest sized basis sets. We reserve the use of large basis sets for the future calculations, when we intend to go beyond the Hartree-Fock level to utilize these Wannier functions to do correlated calculations. The reason we have chosen to compare our results to those obtained using the CRYSTAL program is because not only is CRYSTAL based upon an LCAO formalism employing Gaussian type of basis functions similar to our case, but also it is a well-tested program and widely believed to be the state of the art in crystalline Hartree-Fock calculations²⁰.

All the calculations to be presented below assume the observed face-centered cubic (fcc) structure for the compounds. The reference unit cell \mathcal{C} was taken to be the primitive cell containing an anion at the $(0, 0, 0)$ position and the cation at $(0, 0, a/2)$, where a is the lattice constant. The calculations were performed with different values of the lattice constants to be indicated later. The basis sets used for lithium, fluorine and chlorine are shown in tables I, II and III, respectively. For lithium we adopted the basis set of Dovesi et al. used in their lithium hydride study²¹, while for fluorine and chlorine basis sets originally published by Huzinaga and collaborators²² were used. The values of the level-shift parameters λ_γ^k 's of Eq.(12) should be high enough to guarantee sufficient orthogonality while still allowing for numerical stability. Thus this choice leaves sufficient room for experimentation. We found

the values in the range $\approx 1.0 \times 10^3$ — 1.0×10^4 a.u. suitable for our work. We verified by explicit calculations that our results had indeed converged with respect to the values of the shift parameters. In the course of the evaluation of integrals needed to construct the Fock matrix, all the integrals whose magnitudes were smaller than 1.0×10^{-7} a.u. were discarded both in our calculations as well as in the CRYSTAL calculations.

The comparison of our ground-state energies per unit cell with those obtained using the identical basis sets by the CRYSTAL program¹³ is illustrated in tables IV and V for different values of lattice constants. The biggest disagreement between the two types of calculations is 0.7 millihartree. A possible source of this disagreement is our use of lobe functions to approximate the *p*-type CGTFs. However, since the typical accuracy of a CRYSTAL calculation is also 1 millihartree¹³, we consider this disagreement to be insignificant. Such excellent agreement between the total energies obtained using two different approaches gives us confidence as to the essential correctness of our approach. From the results it is also obvious that the basis set used in these calculations is inadequate to predict the lattice constant and the bulk modulus correctly. To be able to do so accurately, one will have to employ a much larger basis set such as the one used by Prencipe et al.¹⁹. Since Hartree-Fock lattice constants generally are much larger than the experimental value, we reserve the large-scale Hartree-Fock calculations for future studies in which we will also go beyond the Hartree-Fock level to include the influence of electron correlations.

Valence Wannier functions for LiF and LiCl are plotted along different crystal directions in Figs. 1, 2, 3 and 4. Lattice constants for these calculations were assigned their experimental values²³ of 3.99 Å and 5.07 Å, for LiF and LiCl, respectively. Although core orbitals were also obtained from the same set of calculations, we have not plotted them here because they are trivially localized. The *p*-character of the Wannier functions is evident from the antisymmetric nature of the plots under reflection. The additional nodes introduced in the orbitals due to their orthogonalization to orbitals centered on the atoms of region \mathcal{N} are also evident. The localized nature of these orbitals is obvious from the fact that the orbitals decay rapidly as one moves away from the atom under consideration. The orthogonality of

the orbitals of the reference cell to those of the neighborhood (region \mathcal{N}) was always better than 1.0×10^{-5} .

Now we discuss the data for x-ray structure factors. These quantities were also evaluated at experimental lattice constants mentioned above. The x-ray structure factors obtained by our method are compared to values calculated with the CRYSTAL program, and experimental data, in tables VI and VII for LiF and LiCl, respectively. For the case of LiF we directly compare the theoretical values with the experimental data of Merisalo et al.²⁴, extrapolated to zero temperature by Euwema et al.²⁵. For LiCl it was not possible for us to extrapolate the experimental data of Inkinen et al.²⁶, measured at $T = 78\text{ K}$, to the corresponding zero temperature values. Therefore, to compare our LiCl calculations to the experiment, we correct our theoretical values for thermal motion using the Debye-Waller factors of $B_{\text{Li}} = 0.93\text{\AA}^2$ and $B_{\text{Cl}} = 0.41\text{\AA}^2$, measured also by Inkinen et al.²⁶ The Debye-Waller corrections were applied to the individual form factors of Li^+ and Cl^- ions. From both the tables it is obvious that our results are in almost exact agreement with those of CRYSTAL. This implies that our Wannier function HF approach based description of the charge density of systems considered here, is identical to a Bloch orbital based HF description as formulated in CRYSTAL¹³. For the case of LiF the agreement between our results and the experiment is also quite good, maximum errors being $\approx 5\%$. For the case of LiCl, our corrected values of x-ray structure factors deviate from the experimental values at most by approximately 3%. Perhaps by using a larger basis set one can obtain even better agreement with experiments.

Finally we turn to the discussion of Compton profiles. Directional and isotropic Compton profiles, computed using our approach and the CRYSTAL program, are compared to the isotropic Compton profiles measured by Paakkari et al.²⁷, in tables VIII and IX. We obtain the isotropic Compton profiles from our directional profiles by performing a directional average of the profiles along the three crystal directions according to the formula $\langle J \rangle = \frac{1}{26}(6J_{100} + 12J_{110} + 8J_{111})$ valid for an fcc lattice²⁸. While experimental data for directional Compton profiles exist in the case of LiF²⁸, no such measurements have been performed for LiCl, to the best of our knowledge. For LiF there is close agreement between our

results and the ones calculated using the CRYSTAL program. For LiCl our results disagree with the CRYSTAL results somewhat for small values of momentum transfer, although relatively speaking the disagreement is quite small—the maximum deviation being $\approx 0.3\%$ for $q = 0.0$ and the $[100]$ direction. The possible source of the disagreement may be that to get the values of Compton profiles for all the desired values of momentum transfer, we had to use the option of CRYSTAL¹³ where the Compton profiles are obtained by using the real-space density matrix rather than its more accurate \mathbf{k} -space counterpart. However, as is clear from the tables, even for those worst cases, there is no significant difference between the averaged out isotropic Compton profiles obtained in our computations and those obtained from CRYSTAL. At the larger values of momentum transfer, our results are virtually identical to the CRYSTAL results. The close agreement with CRYSTAL clearly implies that our Wannier function based description of the momentum distribution of the electrons in the solid is identical to the one based upon Bloch orbitals.

Considering the fact that we have used a rather modest basis set, it is quite surprising that the values of isotropic Compton profiles obtained by us are in close agreement with the corresponding experimental values²⁷. An inspection of tables VIII and IX reveals that the calculated values always agree with the experimental ones to within 6%. However, ours as well as the CRYSTAL calculations presented here are not able to describe the observed anisotropies in the directional Compton profiles²⁸ for LiF which is also the reason that we have not compared the theoretical anisotropies to the experimental ones. For small values of momentum transfer the calculated values are even in qualitative disagreement with the experimental results, although for large momentum transfer the qualitative agreement is restored. This result is not surprising, however, because, as Berggren et al. have argued²⁸ in their detailed study, the proper description of the Compton anisotropy mandates a good description of the long-range tails of the crystal orbitals. To be able to do so with the Gaussian-type of basis functions used here, one will—unlike the present study—have to include basis functions with quite diffuse exponents.

IV. CONCLUSIONS

In conclusion, an *ab initio* Hartree-Fock approach for an infinite insulating crystal which yields orbitals in a localized representation has been discussed in detail. It was applied to compute the total energies per unit cell, x-ray structure factors and directional Compton profiles of two halides of lithium, LiF and LiCl. The close agreement between the results obtained using the present approach, and the ones obtained using the conventional Bloch orbital based HF approach, demonstrates that the two approaches are entirely equivalent. The advantage of our approach is that by considering local perturbations to the Hartree-Fock reference state by conventional quantum-chemical methods, one can go beyond the mean-field level and study the influence of electron correlations on an infinite solid in an entirely *ab initio* manner. Presently projects along this direction are at progress in our group, and in a future publication we will study the influence of electron correlations on the ground state of a solid.

ACKNOWLEDGMENTS

One of us (A.S.) gratefully acknowledges useful discussions with Prof. Roberto Dovesi, and his help regarding the use of the CRYSTAL program.

APPENDIX A: INTEGRAL EVALUATION

In this section we discuss the calculation of various terms in the Fock matrix. Since the kinetic-energy matrix elements $T_{pq} = \langle p|T|q \rangle$ and the overlap-matrix elements $S_{pq} = \langle p|q \rangle$ have simple mathematical expressions and are essentially unchanged from molecular calculations, we will not discuss them in detail. However, we will consider the evaluation of the rest of the contributions to the Fock matrix at some length.

1. Nuclear Attraction Integrals

The electron-nucleus attraction term of the Fock matrix contains the infinite lattice sums involving the attractive interaction acting on the electrons of the reference cell due to the infinite number of nuclei in the solid. When treated individually, this term is divergent. However, when combined with the Coulombic part of the electron repulsion to be discussed in the next section, convergence is achieved because the divergences inherent in both sums cancel each other owing to the opposite signs. This fact is a consequence of the charge neutrality of the unit cell and is used in the Ewald-summation technique³⁰ to make the individual contributions also convergent by subtracting, from the corresponding potential a shadow potential emerging from a fictitious homogeneous charge distribution of opposite sign. In addition, in the Ewald method, one splits the lattice potential into a short-range part whose contribution is rapidly convergent in the \mathbf{r} -space and a long-range part which converges fast in \mathbf{k} -space. Therefore, in the Ewald-summation technique one replaces the electron-nucleus interaction potential due to a lattice composed of nuclei of charge Z , by the effective potential³⁰

$$U^{Ew}(\mathbf{r}) = -Z \left\{ \sum_{\mathbf{R}_i} \frac{\text{erfc}(\sqrt{\lambda}|\mathbf{r} - \mathbf{R}_i|)}{|\mathbf{r} - \mathbf{R}_i|} + \frac{4\pi}{\omega} \sum_{\mathbf{K}_i \neq 0} \frac{\exp(-\frac{\mathbf{K}_i^2}{4\lambda} + i\mathbf{K}_i \cdot \mathbf{r})}{\mathbf{K}_i^2} - \frac{\pi}{\omega \lambda} \right\}, \quad (\text{A1})$$

where \mathbf{R}_i represents the positions of the nuclei on the lattice, \mathbf{K}_i are the vectors of the reciprocal lattice, ω is the volume of the unit cell, λ is a convergence parameter to be discussed later and erfc represents the complement of the error function. Matrix elements of the Ewald potential of Eq.(A1) with respect to primitive s -type basis functions were derived by Stoll³¹ to be

$$U_{pq}^{Ew}(\mathbf{R}_p, \mathbf{R}_q) = \langle p(\mathbf{R}_p) | U^{Ew} | q(\mathbf{R}_q) \rangle = \hat{U}_{pq} S_{pq}. \quad (\text{A2})$$

Above p and q label the primitive basis functions, \mathbf{R}_p and \mathbf{R}_q represent the positions of the unit cells in which they are located and S_{pq} represents the overlap matrix element between the two primitives given by

$$S_{pq} = \frac{2^{3/2}(\eta_p\eta_q)^{3/4}}{(\eta_p + \eta_q)^{3/2}} \exp(-A_{pq}(\mathbf{r}_p + \mathbf{R}_p - \mathbf{r}_q - \mathbf{R}_q)^2). \quad (\text{A3})$$

The vectors \mathbf{r}_p and \mathbf{r}_q above specify the centers of the two basis functions relative to the origin of the unit cell, η_p and η_q represent the exponents of the two Gaussians, $A_{pq} = \frac{\eta_p\eta_q}{\eta_p + \eta_q}$ and

$$\hat{U}_{pq} = -ZW(C_{pq}, \mathbf{r}_{p,q}), \quad (\text{A4})$$

with $C_{pq} = \eta_p + \eta_q$, $\mathbf{r}_{p,q} = \{\eta_p(\mathbf{r}_p + \mathbf{R}_p) + \eta_q(\mathbf{r}_q + \mathbf{R}_q)\}C_{pq}^{-1}$ and

$$W(\alpha, \mathbf{r}) = \sum_{\mathbf{R}_i} \frac{\text{erfc}(\sqrt{\epsilon}|\mathbf{r} - \mathbf{R}_i|) - \text{erfc}(\sqrt{\alpha}|\mathbf{r} - \mathbf{R}_i|)}{|\mathbf{r} - \mathbf{R}_i|} + \frac{4\pi}{\omega} \sum_{\mathbf{K}_i \neq 0} \frac{\exp(-\frac{\mathbf{K}_i^2}{4\epsilon} + i\mathbf{K}_i \cdot \mathbf{r})}{\mathbf{K}_i^2} - \frac{\pi}{\omega} \left(\frac{1}{\epsilon} - \frac{1}{\alpha} \right). \quad (\text{A5})$$

where the parameter ϵ takes over the role of the convergence parameter λ of Eq.(A1). The remaining quantities are the the same as those in Eq.(A1). It is clear that the function $W(\alpha, \mathbf{r})$ involves lattice sums both in the direct space and the reciprocal space. Although the final value of the function will be independent of the choice of the convergence parameter ϵ , both these sums can be made to converge optimally by making a judicious choice of it. Large values of ϵ lead to faster convergence in the real space but to slower one in the reciprocal space and with smaller values of ϵ the situation is just the opposite. Therefore, for optimal performance, the choice of ϵ is made dependent on the value of α . In the present work we make the choice so that if $\alpha > \frac{\pi}{\omega^{2/3}}$, $\epsilon = \frac{\pi}{\omega^{2/3}}$ and if $\alpha \leq \frac{\pi}{\omega^{2/3}}$, $\epsilon = \alpha$. In the former case the sum is both, in the real and the reciprocal space while in the latter case the sum is entirely in the reciprocal space. Although we have written an efficient computer code to evaluate the function $W(\alpha, \mathbf{r})$, it remains the most computer intensive part of our program.

The computational effort involved in the computation of these integrals can be reduced by utilizing the translational symmetry. One can verify that as a consequence of translation symmetry

$$U_{pq}^{Ew}(\mathbf{R}_p, \mathbf{R}_q) = U_{pq}^{Ew}(\mathbf{t}_{pq}, o) = U_{pq}^{Ew}(\mathbf{t}_{pq}), \quad (\text{A6})$$

where $\mathbf{t}_{pq} = \mathbf{R}_p - \mathbf{R}_q$ is also a vector of the direct lattice, o represents the reference unit cell and the last term is a compact notation for the second term. Since the number of unique \mathbf{t}_{pq} vectors is much smaller than the number of pairs $(\mathbf{R}_p, \mathbf{R}_q)$, the use of Eq.(A6) reduces the computational effort considerably. To further reduce the computational effort we also use the interchange symmetry

$$U_{pq}^{Ew}(\mathbf{t}_{pq}) = U_{qp}^{Ew}(-\mathbf{t}_{pq}) . \quad (\text{A7})$$

Additional savings are achieved if one realizes that matrix elements $U_{pq}^{Ew}(\mathbf{t}_{pq})$ become smaller as larger the distance $|\mathbf{t}_{pq}|$ between the interacting charge distributions becomes. As is clear from Eq.(A2), a good estimate of the magnitude of an integral is the overlap element S_{pq} ²⁹. Therefore, we compute only those integrals whose overlap elements S_{pq} are larger than some threshold t_n . In the present calculations we chose $t_n = 1.0 \times 10^{-7}$.

2. Electronic Coulomb Integrals

To calculate the Coulomb contribution to the Fock matrix, one needs to evaluate the two-electron integrals with infinite lattice sum

$$J_{pq;rs}(\mathbf{R}_p, \mathbf{R}_q, \mathbf{R}_r, \mathbf{R}_s) = \sum_k \langle p(\mathbf{R}_p) r(\mathbf{R}_r + \mathbf{R}_k) | \frac{1}{r_{12}} | q(\mathbf{R}_q) s(\mathbf{R}_s + \mathbf{R}_k) \rangle , \quad (\text{A8})$$

where p, q, r and s represent the primitive basis functions and $\mathbf{R}_p, \mathbf{R}_q, \mathbf{R}_r$ and \mathbf{R}_s represent the unit cells in which they are centered. This integral, treated on its own is divergent, as discussed in the previous section. However, using the Ewald-summation technique, one can make this series conditionally convergent with the implicit assumption that its divergence will cancel the corresponding divergence of the electron nucleus interaction. Since the details of the Ewald-summation technique for the Coulomb part of electron repulsion are essentially identical to the case of electron-nucleus interaction, we will just state the final results³¹

$$\tilde{J}_{pq;rs}(\mathbf{R}_p, \mathbf{R}_q, \mathbf{R}_r, \mathbf{R}_s) = S_{pq} S_{rs} W(B_{rs}^{pq}, \mathbf{r}_{p,q}^{r,s}) \quad (\text{A9})$$

where

$$(B_{rs}^{pq})^{-1} = (\eta_p + \eta_q)^{-1} + (\eta_r + \eta_s)^{-1} ,$$

and

$$\mathbf{r}_{p,q}^{r,s} = \mathbf{r}_{r,s} - \mathbf{r}_{p,q} .$$

All the notations used in the equations above were defined in the previous section. The expression $\tilde{J}_{pq;rs}$ used in Eq.(A9), as against $J_{pq;rs}$ of Eq.(A8), is meant to remind us that the matrix elements stated in Eq.(A9) are those of the two-electron Ewald potential and not those of the ordinary Coulomb potential.

Like in the case of electron-nucleus attraction, one can utilize the translational symmetry for the present case to reduce the computational effort significantly. The corresponding relations in the present case are

$$\tilde{J}_{pq;rs}(\mathbf{R}_p, \mathbf{R}_q, \mathbf{R}_r, \mathbf{R}_s) = \tilde{J}_{pq;rs}(\mathbf{t}_{pq}, o, \mathbf{t}_{rs}, o) = \tilde{J}_{pq;rs}(\mathbf{t}_{pq}, \mathbf{t}_{rs}), \quad (\text{A10})$$

where as before o represents the reference unit cell, $\mathbf{t}_{pq} = \mathbf{R}_p - \mathbf{R}_q$, $\mathbf{t}_{rs} = \mathbf{R}_r - \mathbf{R}_s$ and the last term in Eq.(A10) is a compact notation for the second term. Since the number of pairs $(\mathbf{t}_{pq}, \mathbf{t}_{rs})$ is much smaller than the number of quartets $(\mathbf{R}_p, \mathbf{R}_q, \mathbf{R}_r, \mathbf{R}_s)$, use of Eq.(A10) results in considerable savings of computer time and memory. In addition, we also use the four interchange relations of the form of Eq.(A7) to further reduce the number of nonredundant integrals. Additionally, these integrals also satisfy the interchange relation

$$\tilde{J}_{pq;rs}(\mathbf{t}_{pq}, \mathbf{t}_{rs}) = \tilde{J}_{rs,pq}(\mathbf{t}_{rs}, \mathbf{t}_{pq}) . \quad (\text{A11})$$

To keep the programming simple, however, at present we do not utilize this symmetry. In future, we do intend to incorporate this symmetry in the code.

Similar to the case of electron-nucleus integrals, here also we use the magnitude of the product $S_{pq}S_{rs}$ to estimate the size of the integral to be computed and proceed with its calculation only if it is greater than a threshold t_c , taken to be 1.0×10^{-7} in this study.

3. Electronic Exchange Integrals

In order to compute the exchange contribution to the Fock matrix, one has to compute the following two-electron integrals involving infinite lattice sum

$$K_{pq;rs}(\mathbf{R}_p, \mathbf{R}_q, \mathbf{R}_r, \mathbf{R}_s) = \sum_k \langle p(\mathbf{R}_p) s(\mathbf{R}_s + \mathbf{R}_k) | \frac{1}{r_{12}} | r(\mathbf{R}_r + \mathbf{R}_k) q(\mathbf{R}_q) \rangle, \quad (\text{A12})$$

where the notation is identical to the previous two cases. By using the translational symmetry arguments one can show even for the exchange case that

$$K_{pq;rs}(\mathbf{R}_p, \mathbf{R}_q, \mathbf{R}_r, \mathbf{R}_s) = K_{pq;rs}(\mathbf{t}_{pq}, o, \mathbf{t}_{rs}, o) = K_{pq;rs}(\mathbf{t}_{pq}, \mathbf{t}_{rs}), \quad (\text{A13})$$

where the last term in Eq.(A13) above is a compact notation for the second term. As in the previous two cases, the use of translational symmetry results in considerable savings of computer time and storage. Explicitly

$$K_{pq;rs}(\mathbf{t}_{pq}, \mathbf{t}_{rs}) = \sum_k \langle p(\mathbf{t}_{pq}) s(\mathbf{R}_k) | \frac{1}{r_{12}} | r(\mathbf{t}_{rs} + \mathbf{R}_k) q(o) \rangle. \quad (\text{A14})$$

Although Eq.(A14) contains an infinite sum over lattice vectors \mathbf{R}_k , the contributions of each of the terms decreases rapidly with the increasing distances $|\mathbf{t}_{rs} + \mathbf{R}_k - \mathbf{t}_{pq}|$ and $|\mathbf{R}_k|$ between the interacting charge distributions. A good estimate of the contribution of the individual terms is provided by the product of overlap matrix elements between the interacting charge distributions namely, $S_{pr} = \langle p(\mathbf{t}_{pq}) | r(\mathbf{t}_{rs} + \mathbf{R}_k) \rangle$ and $S_{qs} = \langle q(o) | s(\mathbf{R}_k) \rangle$ ²⁹. Therefore, in the computer implementation, we arrange the vectors \mathbf{R}_k so that the corresponding overlaps are in the descending order and the loop involving the sum over \mathbf{R}_k in Eq.(A14) is terminated once the individual overlap matrix elements or their product are less than a specified threshold t_e . The computer code for evaluating these integrals is a modified version of the program written originally by Ahlrichs²⁹. The value of the threshold t_e used in these calculations was 1.0×10^{-7} . The exchange integrals also satisfy interchange symmetries similar to those of Eqs.(A7) and (A11), which are not used in the present version of the code for the ease of programming. In future, however, we plan to use them as well.

As described above, to minimize the need of computer time and storage, we have made extensive use of translational symmetry. However, the integral evaluation can be further optimized considerably by making use of point group symmetry as is done in the CRYSTAL program¹³. Implementation of point group symmetry, as well as the use of CGTOs instead of lobe-type functions, is planned for future improvements of the present code.

REFERENCES

[†] e-mail address: shukla@mpipks-dresden.mpg.de

¹ G. Wannier, Phys. Rev. **52**, 191 (1937).

² W. Kohn, Phys. Rev. B **7**, 4388 (1973).

³ G. Galli and M. Parrinello, Phys. Rev. Lett. **69**, 3547 (1992); F. Mauri, G. Galli and R. Car, Phys. Rev. B **47**, 9973 (1993); P. Ordejón, D.A. Drabold, M.P. Grumbach and R.M. Martin, Phys. Rev. B **48**, 14646 (1993); F. Mauri, G. Galli, Phys. Rev. B **50**, 4316 (1994); E. Hernández, M.J. Gillan and C.M. Goringe, Phys. Rev. B **53**, 7147 (1996).

⁴ R.W. Nunes and D. Vanderbilt, Phys. Rev. Lett. **73**, 712 (1994).

⁵ We use the term “conventional quantum-chemical methods” to denote the approaches which deal with the many-particle wave function of the system rather than with its charge and spin density only. These include configuration interaction, coupled-cluster, projection technique and the many-body perturbation theory based approaches. For a review of these methods and their applications to solid-state theory see, e.g., P. Fulde, Springer Series in Solid-State Sciences, Vol. 100, Electron Correlations in Molecules and Solids, 3rd edn. (Springer, Berlin, 1995).

⁶ J.M. Foster and S.F. Boys, Rev. Mod. Phys. **32**, 300 (1960); C. Edmiston and K. Ruedenberg, Rev. Mod. Phys. **35** 457 (1963); T. L. Gilbert, in: *Molecular Orbitals in Chemistry, Physics and Biology*, ed. P.O. Löwdin and B. Pullman (Academic, New York, 1964), pp. 405-420; W.H. Adams, J. Chem. Phys. **34**, 89 (1961); *ibid.* **37**, 2009 (1962); *ibid.* **42**, 4030 (1965); J. Pipek and P.G. Mezey, J. Chem. Phys. **90**, 4916 (1989).

⁷ A.B. Kunz and D.L. Klein, Phys. Rev. B **17**, 4614 (1978); A.B. Kunz, Phys. Rev. B **26**, 2056 (1982); A.B. Kunz and J.M. Vail, Phys. Rev. B **38**, 1058 (1988).

⁸ For a review see, J.M. Vail, R. Pandey and A.B. Kunz Rev. Solid State Sciences, **5**, 241 (1991).

- ⁹ A.B. Kunz, J. Meng and J.M. Vail, Phys. Rev. B **38**, 1064 (1988).
- ¹⁰ H. Stoll, Phys. Rev. B **46**, 6700 (1992); Chem. Phys. Letters **191**, 548 (1992).
- ¹¹ J. Gräfenstein, H. Stoll and P. Fulde, Chem. Phys. Lett. **215**, 611 (1993); B. Paulus, P. Fulde and H. Stoll, Phys. Rev. B **51**, 10572 (1995); K. Doll, M. Dolg, P. Fulde and H. Stoll Phys. Rev. B **52**, 4842 (1995); B. Paulus, P. Fulde and H. Stoll, Phys. Rev. B **54**, 2556 (1996); K. Doll, M. Dolg and H. Stoll Phys. Rev. B **54**, 13529 (1996); S. Kalvoda, B. Paulus, P. Fulde and H. Stoll, Phys. Rev. B **55**, 4027 (1997); B. Paulus, F.-J. Shi and H. Stoll, J. Phys. Cond. Matter **9**, 2745 (1997); K. Doll, M. Dolg, P. Fulde and H. Stoll, Phys. Rev. B **55**, 10282 (1997); M. Albrecht, B. Paulus and H. Stoll, Phys. Rev. B (to be published); K. Doll, H. Stoll, Phys. Rev. B (to be published).
- ¹² A. Shukla, M. Dolg, H. Stoll and P. Fulde, Chem. Phys. Lett. **262**, 213 (1996).
- ¹³ R. Dovesi, C. Pisani, C. Roetti, M. Causa and V.R. Saunders, CRYSTAL88, Quantum Chemistry Program Exchange, Program No. 577 (Indiana University, Bloomington, IN 1989); R. Dovesi, V.R. Saunders and C. Roetti, CRYSTAL92 User Document, University of Torino, Torino, and SERC Daresbury Laboratory, Daresbury, UK, (1992).
- ¹⁴ We use the conventional atomic units in which the unit of length is Bohr and the unit of energy is Hartree.
- ¹⁵ The basis functions with $n_x + n_y + n_z = 2$ and higher cannot be characterized as pure spherical harmonics and contain contributions from lower angular momenta as well. For example, $n_x + n_y + n_z = 2$ functions also contain s -type contributions besides the contribution from d -type functions. However, in the quantum-chemistry community, the value of $n_x + n_y + n_z$ is colloquially referred to as the angular momentum of the basis function.
- ¹⁶ In molecular calculations lobe-type functions were developed independently by H. Preuss, Z. Naturf. A **11** (1956) 823 and J.L. Whitten, J. Chem. Phys. **39**, 349 (1963). Their use in solid-state calculations within the context of Bloch-orbital based Hartree-Fock calculations

was pioneered by Euwema and coworkers. See, for example, R.N. Euwema, D.L. Wilhite and G.T. Surrat, Phys. Rev. B **7**, 818 (1973).

¹⁷ Usually in quantum-chemistry literature the contribution of the two spin projections is absorbed in the density matrix and it is defined with a factor of 2 multiplying the right hand side of Eq.(16). However, we have chosen to absorb the contributions of the spin sum in various terms of the Fock matrix and total energy, instead.

¹⁸ P. Eisenberger and P.M. Platzman, Phys. Rev. A **2**, 415 (1970).

¹⁹ M. Prencipe, A. Zupan, R. Dovesi, E. Aprá and V.R. Saunders, Phys. Rev. B **51**, 3391 (1995).

²⁰ The applications of the CRYSTAL program are too numerous to be listed here. For an excellent review of the formalism see C. Pisani, R. Dovesi and C. Roetti, Springer Lecture Notes in Chemistry, Vol. 48, Hartree-Fock ab initio Treatment of Crystalline Systems (Springer, Berlin, 1988).

²¹ R. Dovesi, C. Ermondi, E. Ferrero, C. Pisani, and C. Roetti, Phys. Rev. B **29**, 3591 (1984).

²² The basis sets for F and Cl were taken from the program library of the MOLPRO package. The MOLPRO library attributes the basis set to S. Huzinaga and coworkers. Unfortunately, we have been unable to locate the original reference. MOLPRO is a package of ab initio programs written by H.-J. Werner and P.J. Knowles, with contributions from J. Almlöf, R.D. Amos, M.J.O. Deegan, S.T. Elbert, C. Hampel, W. Meyer, K. Peterson, R. Pitzer, A. J. Stone, and P.R. Taylor.

²³ W.G. Wyckoff, *Crystal Structures*, 2nd ed. (Wiley, New York, 1968), Vol. 1.

²⁴ M. Merisalo and O. Inkinen, Ann. Acad. Sci. Fenn. A6 **207**, 3 (1966).

²⁵ R.N. Euwema, G.G. Wepfer, G.T. Surrat and D.L. Wilhite, Phys. Rev. B **9**, 5249 (1974).

²⁶ O. Inkinen and M. Järvinen, Phys. Kondens. Materie **7**, 372 (1968).

- ²⁷ T. Paakkari and V. Hanolen, Phys. Scripta **17**, 433 (1978).
- ²⁸ W.A. Reed, P. Eisenberger, F. Martino and K.F. Berggren, Phys. Rev. Lett. **35**, 114 (1975); K.F. Berggren, F. Martino, P. Eisenberger, W.A. Reed, Phys. Rev. B **13**, 2292 (1976).
- ²⁹ F. Driessler, R. Ahlrichs, Chem. Phys. Letters **23**, 571 (1973) ; R. Ahlrichs, Theor. Chim. Acta **33**, 157 (1974).
- ³⁰ P.P. Ewald, Ann. Phys. (Leipzig) **64**, 253 (1921).
- ³¹ H. Stoll, Ph.D. thesis, Universität Stuttgart (1974).

FIGURES

FIG. 1. LiF: $2p_z$ -type valence Wannier function centered on F^- (located at origin) plotted along the $\mathbf{r} = x(0, 0, 1)$ direction. Nodes near the $(0, 0, \pm \frac{a}{2})$ positions are due to its orthogonalization to the Li^+ $1s$ orbital located there. All distances are in atomic units.

FIG. 2. LiF: $2p_x$ -type valence Wannier function centered on F^- (located at origin) plotted along the $\mathbf{r} = x(1, 1, 0)$ direction. Nodes near the $(\pm \frac{a}{2}, \pm \frac{a}{2}, 0)$ positions are due to its orthogonalization to $2p$ orbitals of F^- located there. All distances are in atomic units.

FIG. 3. LiCl: $3p_z$ -type valence Wannier function centered on Cl^- (located at origin) plotted along the $\mathbf{r} = x(0, 0, 1)$ direction. Nodes near the origin are due to its orthogonalization to the Cl^- $2p$ -orbitals centered there while those near the $(0, 0, \pm \frac{a}{2})$ positions are due to its orthogonalization to the Li^+ $1s$ orbital located there. All distances are in atomic units.

FIG. 4. LiCl: $3p_x$ -type valence Wannier function centered on Cl^- (located at origin) plotted along the $\mathbf{r} = x(1, 1, 0)$ direction. Nodes near the origin are due to its orthogonalization to the Cl^- $2p$ -orbitals centered there, while the two nodes each near the $(\pm \frac{a}{2}, \pm \frac{a}{2}, 0)$ positions are due to its orthogonalization to both, the $3s$ and the $3p$ orbitals of Cl^- located there. All distances are in atomic units.

TABLES

TABLE I. Exponents and contraction coefficients used in the basis set for lithium²¹.

Shell type	Exponent	Contraction Coefficient
1s	700.0	0.001421
	220.0	0.003973
	70.0	0.016390
	20.0	0.089954
	5.0	0.315646
	1.5	0.494595
2s	0.5	1.0
2p	0.6	1.0

TABLE II. Exponents and contraction coefficients used in the basis set for fluorine²².

Shell type	Exponent	Contraction Coefficient
1s	2931.321	0.005350
	441.9897	0.039730
	100.7312	0.177257
	28.14426	0.457105
2s	8.7256	1.0
3s	1.40145	1.0
4s	0.41673	1.0
2p	10.56917	0.126452
	2.19471	0.478100
3p	0.47911	1.0

TABLE III. Exponents and contraction coefficients used in the basis set for chlorine²².

Shell type	Exponent	Contraction Coefficient
1s	30008.27	0.001471
	4495.692	0.011324
	1021.396	0.056401
	287.6894	0.200188
	92.26777	0.443036
	31.76476	0.402714
2s	7.16468	1.0
3s	2.78327	1.0
4s	0.60063	1.0
5s	0.22246	1.0
2p	157.7332	0.025920
	36.27829	0.164799
	10.84	0.460043
	3.49773	0.499410
3p	0.77581	1.0
4p	0.21506	1.0

TABLE IV. Comparison between between total energies obtained using our approach and those obtained using CRYSTAL¹³ for lithium fluoride for different values of lattice constants. The \mathcal{N} region included up to third-nearest neighbor unit cells. Lattice constants are in units of Å, and energies are in atomic units.

Lattice Constant	Total Energy	
	This work	CRYSTAL
3.8	-106.8985	-106.8980
3.9	-106.8939	-106.8935
3.99	-106.8877	-106.8873
4.1	-106.8780	-106.8774
4.2	-106.8677	-106.8670

TABLE V. Comparison between between total energies obtained using our approach and those obtained using CRYSTAL¹³ for lithium chloride for different values of lattice constants. The \mathcal{N} region included up to third-nearest neighbor unit cells. Lattice constants are in units of Å, and energies are in atomic units.

Lattice Constant	Total Energy	
	This work	CRYSTAL
4.9	-466.5062	-466.5065
5.0	-466.5078	-466.5082
5.07	-466.5080	-466.5085
5.2	-466.5065	-466.5071
5.3	-466.5041	-466.5047

TABLE VI. Calculated and experimental values of x-ray structure factors for LiF in electrons per unit cell. The experimental structure factors are taken from reference²⁴. The Debye-Waller corrections were removed²⁵. The reciprocal-lattice vectors are defined with respect to the conventional cubic unit cell and not the primitive cell. They are labeled by integers h , k and l .

hkl	Experimental	This work	CRYSTAL
111	4.84	5.04	5.04
200	7.74	7.78	7.78
220	5.71	5.68	5.68
311	2.37	2.32	2.32
222	4.61	4.52	4.52
400	3.99	3.84	3.84
331	1.65	1.60	1.60
420	3.46	3.35	3.35
422	3.07	2.99	2.99
511	1.38	1.34	1.33
333	1.38	1.33	1.33
440	2.58	2.52	2.52
531	1.28	1.22	1.22
600	2.41	2.36	2.35
442	2.41	2.35	2.35
620	2.24	2.22	2.22

TABLE VII. Calculated and experimental values of x-ray structure factors for LiCl in electrons per unit cell. Second and third columns report the theoretical values obtained by the specified method, without including the Debye-Waller corrections. Next column reports the theoretical values after including the Debye-Waller factors of $B_{\text{Li}} = 0.93 \text{ \AA}^2$ and $B_{\text{Cl}} = 0.41 \text{ \AA}^2$ corresponding to a temperature $T = 78 \text{ K}^{26}$. Last column reports experimental values of x-ray structure factors measured at $T = 78 \text{ K}^{26}$. The reciprocal-lattice vectors are defined with respect to the conventional cubic unit cell and not the primitive cell. They are labeled by integers h , k and l .

hkl	Uncorrected		Debye-Waller Corrected	
	This Work	CRYSTAL	This work	Experimental
111	11.28	11.28	11.18	10.91
200	13.96	13.96	13.70	13.77
220	11.46	11.46	11.04	11.03
311	7.55	7.55	7.30	7.44
222	10.20	10.20	9.64	9.76
400	9.43	9.44	8.76	8.95
331	6.61	6.62	6.23	6.24
420	8.87	8.88	8.09	8.15
422	8.43	8.43	7.55	7.60
511	6.15	6.16	5.64	5.61
333	6.15	6.16	5.64	5.61
440	7.73	7.74	6.69	6.70
531	5.81	5.81	5.17	5.30
600	7.44	7.44	6.32	6.53
442	7.43	7.44	6.32	6.53
620	7.16	7.17	5.99	5.95

TABLE VIII. Theoretical HF directional Compton profiles for LiF of this work (J_{TW}) compared to those of CRYSTAL (J_{CR}). The directionally averaged Compton profiles of both the approaches ($\langle J_{TW} \rangle$ and $\langle J_{CR} \rangle$) are also compared to the experimental isotropic Compton profiles (J_{exp})²⁷. The Compton profiles and momentum transfer q are in atomic units. The column headings $[hkl]$ refer to the direction of momentum transfer in the crystal. All the profiles are normalized to 5.865 electrons in the interval $q = 0 - 7$ a.u.

q	[100]		[110]		[111]		average		J_{exp}
	J_{TW}	J_{CR}	J_{TW}	J_{CR}	J_{TW}	J_{CR}	$\langle J_{TW} \rangle$	$\langle J_{CR} \rangle$	
0.0	3.759	3.762	3.762	3.760	3.777	3.774	3.766	3.764	3.832
0.1	3.741	3.743	3.749	3.746	3.762	3.759	3.751	3.749	3.814
0.2	3.689	3.691	3.707	3.705	3.718	3.715	3.706	3.705	3.765
0.3	3.609	3.609	3.638	3.636	3.644	3.641	3.633	3.632	3.684
0.4	3.504	3.504	3.541	3.540	3.542	3.540	3.532	3.531	3.574
0.5	3.382	3.382	3.416	3.415	3.413	3.411	3.407	3.406	3.434
0.6	3.245	3.245	3.266	3.266	3.258	3.257	3.259	3.258	3.271
0.7	3.095	3.094	3.094	3.093	3.081	3.081	3.090	3.090	3.089
0.8	2.929	2.928	2.901	2.901	2.886	2.887	2.903	2.903	2.886
0.9	2.745	2.745	2.692	2.692	2.677	2.678	2.700	2.700	2.662
1.0	2.541	2.541	2.472	2.473	2.458	2.460	2.484	2.485	2.426
1.2	2.078	2.077	2.022	2.025	2.020	2.022	2.035	2.036	1.948
1.4	1.608	1.606	1.606	1.607	1.616	1.618	1.610	1.610	1.530
1.6	1.224	1.224	1.261	1.260	1.275	1.276	1.257	1.257	1.202
1.8	0.957	0.956	0.994	0.995	1.003	1.003	0.988	0.988	0.955
2.0	0.772	0.771	0.797	0.797	0.795	0.795	0.790	0.791	0.778
3.0	0.339	0.338	0.324	0.325	0.329	0.329	0.329	0.329	0.336
3.5	0.236	0.236	0.244	0.244	0.241	0.240	0.241	0.241	0.243
4.0	0.179	0.179	0.181	0.181	0.182	0.182	0.181	0.181	0.188

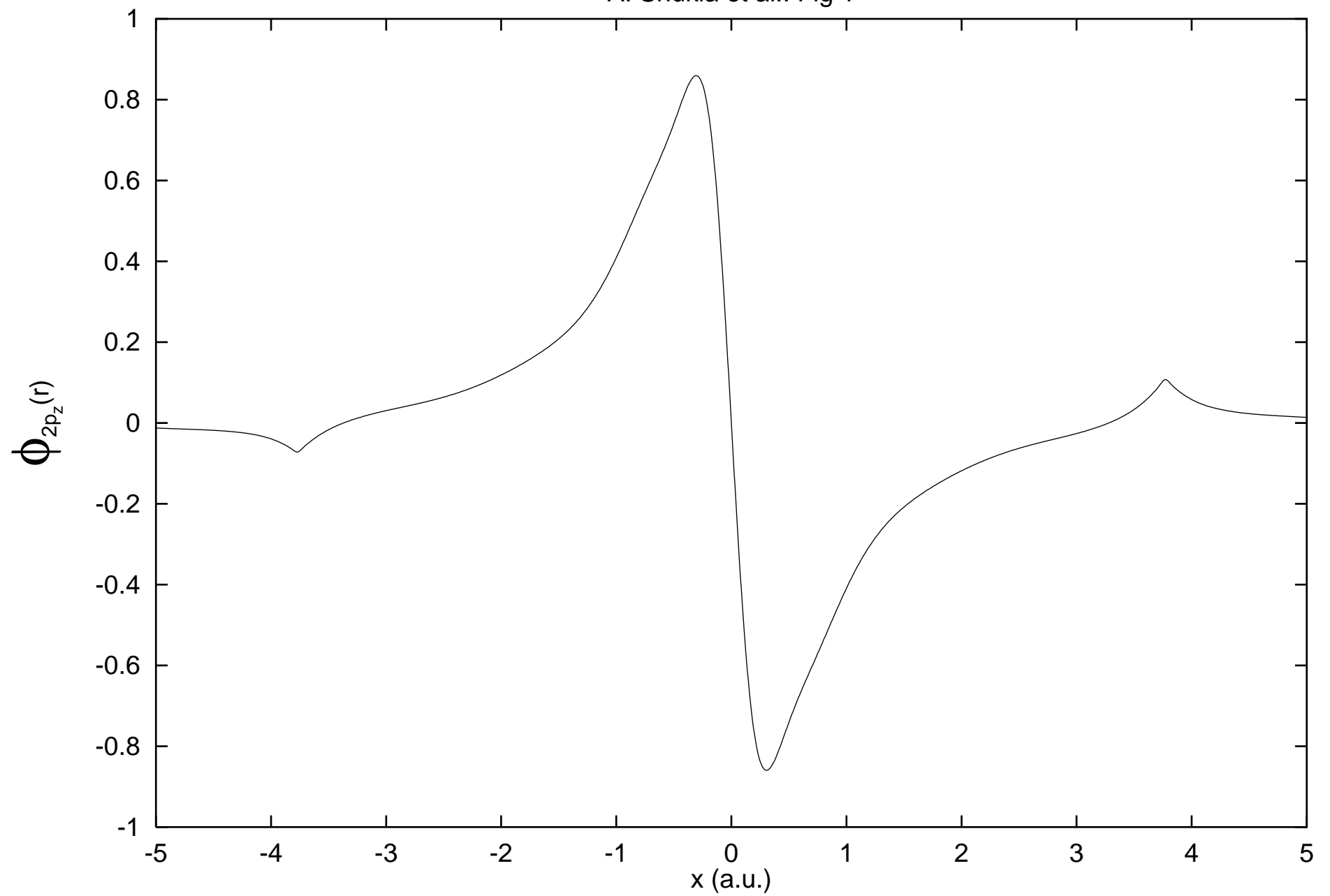
5.0	0.112	0.113	0.113	0.113	0.112	0.112	0.113	0.113	0.115
6.0	0.074	0.074	0.074	0.074	0.074	0.074	0.074	0.074	0.077
7.0	0.050	0.050	0.050	0.050	0.050	0.050	0.050	0.050	0.051

TABLE IX. Theoretical HF directional Compton profiles for LiCl of this work (J_{TW}) compared to those of CRYSTAL (J_{CR}). The directionally averaged Compton profiles of both the approaches ($\langle J_{TW} \rangle$ and $\langle J_{CR} \rangle$) are also compared to the experimental isotropic Compton profiles (J_{exp})²⁷. The Compton profiles and momentum transfer q are in atomic units. The column headings $[hkl]$ refer to the direction of momentum transfer in the crystal. All the profiles are normalized to 9.365 electrons in the interval $q = 0 - 7$ a.u.

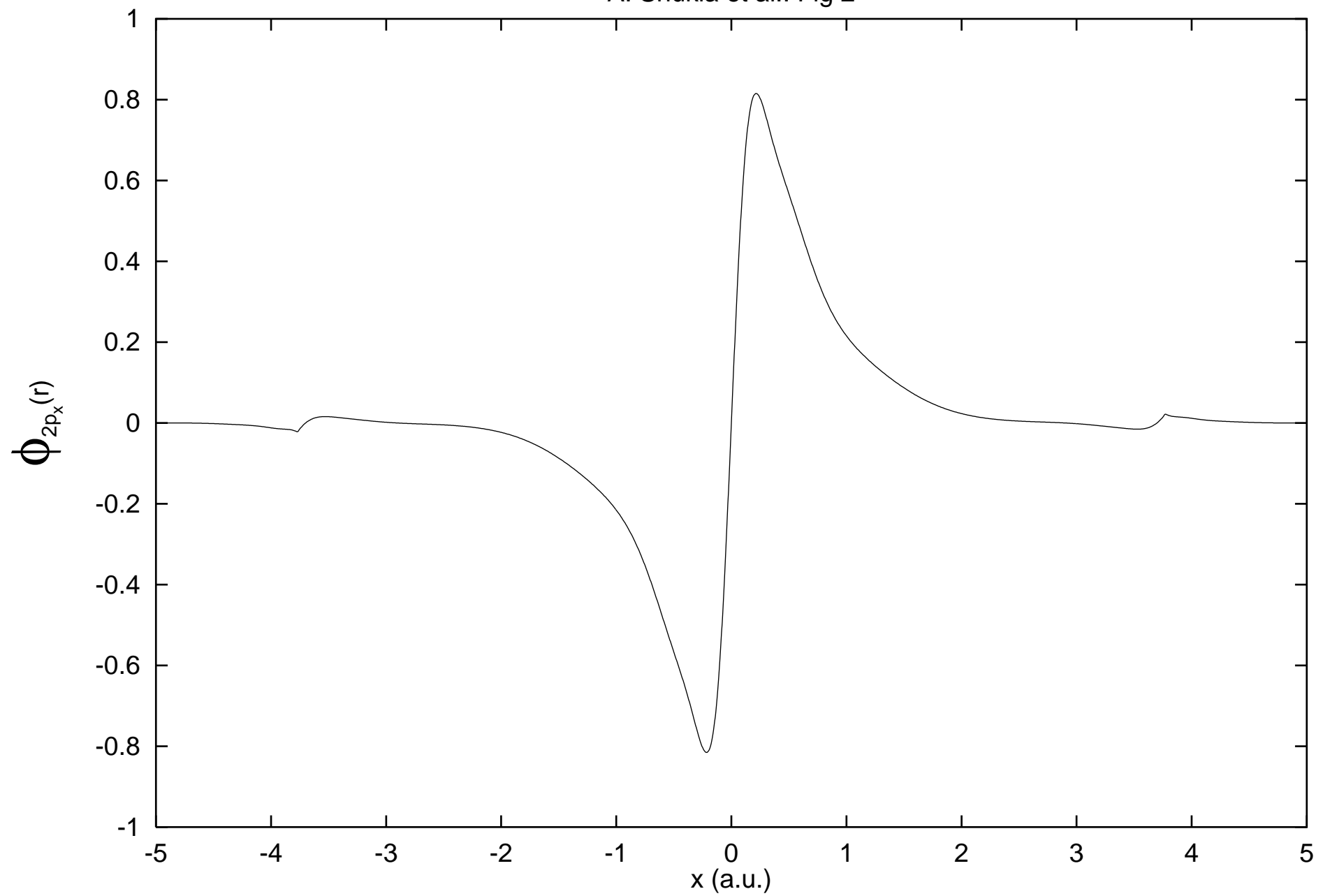
q	[100]		[110]		[111]		average		J_{exp}
	J_{TW}	J_{CR}	J_{TW}	J_{CR}	J_{TW}	J_{CR}	$\langle J_{TW} \rangle$	$\langle J_{CR} \rangle$	
0.0	6.190	6.209	6.207	6.198	6.217	6.204	6.206	6.202	6.282
0.1	6.152	6.169	6.173	6.166	6.181	6.169	6.171	6.168	6.228
0.2	6.041	6.051	6.066	6.065	6.073	6.064	6.062	6.062	6.100
0.3	5.861	5.864	5.881	5.883	5.892	5.887	5.879	5.880	5.896
0.4	5.613	5.607	5.617	5.619	5.634	5.633	5.622	5.620	5.613
0.5	5.297	5.286	5.289	5.286	5.302	5.305	5.295	5.292	5.262
0.6	4.919	4.910	4.903	4.900	4.903	4.908	4.907	4.904	4.857
0.7	4.488	4.486	4.472	4.473	4.452	4.457	4.469	4.471	4.416
0.8	4.023	4.028	4.007	4.014	3.972	3.978	4.000	4.006	3.958
0.9	3.544	3.552	3.528	3.539	3.493	3.500	3.521	3.530	3.512
1.0	3.081	3.086	3.065	3.075	3.046	3.053	3.063	3.071	3.100
1.2	2.309	2.308	2.304	2.305	2.326	2.328	2.312	2.313	2.403
1.4	1.817	1.817	1.827	1.825	1.850	1.848	1.832	1.830	1.897
1.6	1.534	1.532	1.549	1.545	1.548	1.546	1.545	1.542	1.570
1.8	1.350	1.347	1.361	1.358	1.349	1.347	1.355	1.352	1.374
2.0	1.213	1.212	1.210	1.211	1.206	1.204	1.210	1.209	1.227
3.0	0.778	0.777	0.775	0.777	0.776	0.776	0.776	0.776	0.770
3.5	0.630	0.629	0.632	0.630	0.631	0.631	0.631	0.630	0.608
4.0	0.512	0.512	0.510	0.511	0.511	0.511	0.511	0.511	0.487

5.0	0.334	0.333	0.333	0.334	0.334	0.334	0.334	0.334	0.322
6.0	0.224	0.224	0.224	0.225	0.224	0.225	0.224	0.224	0.213
7.0	0.158	0.158	0.157	0.158	0.157	0.158	0.157	0.158	0.151

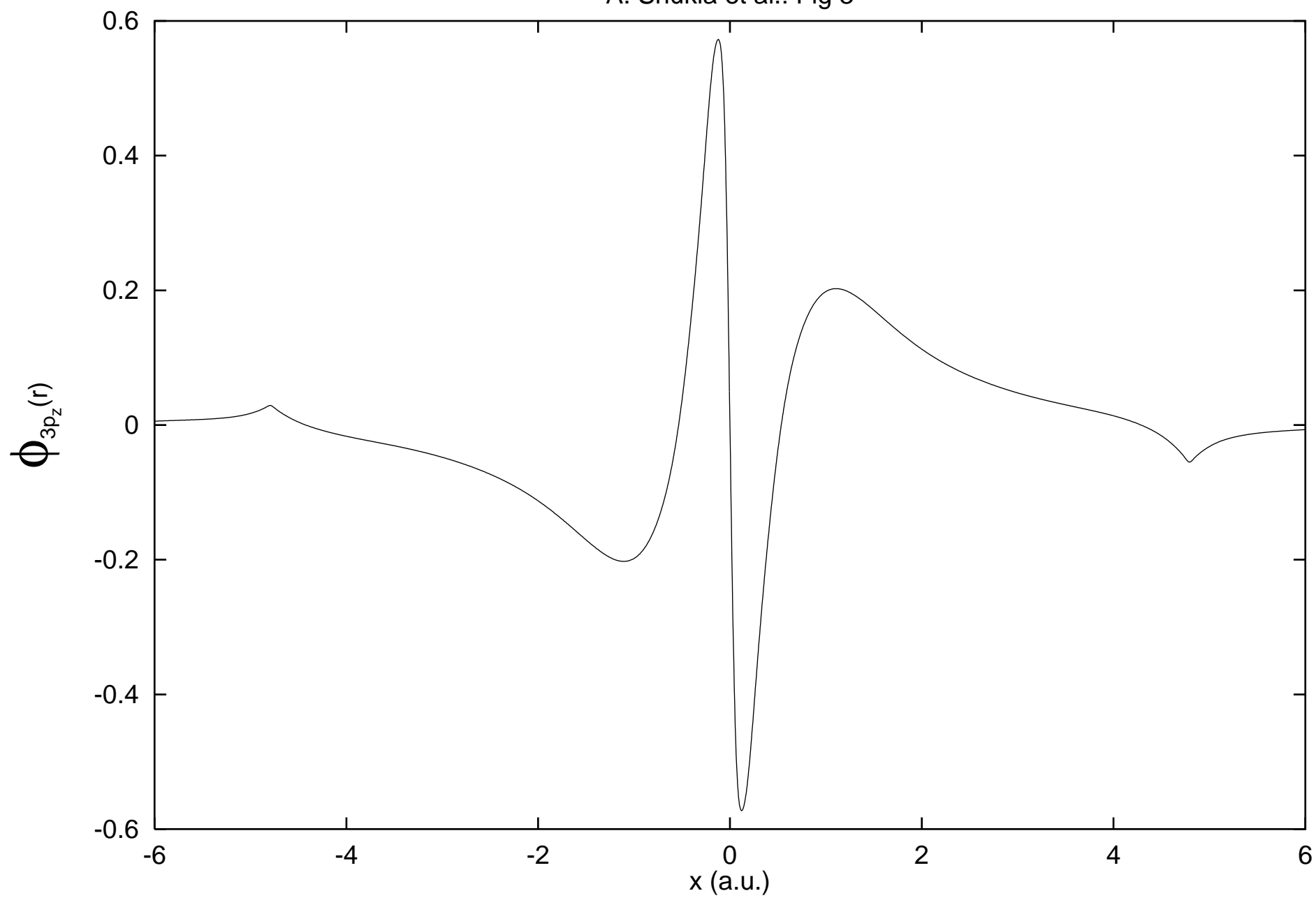
A. Shukla et al.: Fig 1



A. Shukla et al.: Fig 2



A. Shukla et al.: Fig 3



A. Shukla et al.: Fig 4

